FEATURE ARTICLE

Using the Phase of Light as a Photochemical Tool

Robert J. Gordon* and Langchi Zhu

Department of Chemistry (m/c 111), University of Illinois at Chicago, 845 West Taylor Street, Chicago, Illinois 60607-7061

Tamar Seideman

Steacie Institute for Molecular Sciences, National Research Council of Canada, Ottawa K1A 0R6, Canada

Received: October 23, 2000; In Final Form: January 17, 2001

It is shown both theoretically and experimentally that the phase of a transition dipole matrix element may be determined from the interference between competing quantum mechanical paths. Specifically, we consider simultaneous *m*- and *n*-photon excitation of a molecule to a degenerate continuum state, leading to multiple reaction products. Variation of the relative phase of the electromagnetic fields produces a modulation of the product signals in the various channels. A relation between the phase lag between a pair of product signals and properties of the continuum is established. Information is revealed about coupling mechanisms, the properties of weak spectroscopic transitions, and the phases of quasi-bound wave functions.

1. Introduction

The relative phases of wave functions are fundamental physical quantities that may be revealed in interference experiments. They play important roles in quantum control experiments, as, for example, in the sculpting of electronic[1] and vibrational[2] wave packets and as a diagnostic in the use of multipath interference to control reaction branching ratios.[3,4] In the latter case a phase lag between two product channels provides a signature of channel control that could be used to maximize the product branching ratio. In the present review we show how the phase lag is not only a powerful tool for controlling chemical reactions but also contains valuable information about the continuum properties of atoms and molecules.

In conventional photochemical experiments the phases of transition dipole matrix elements cannot be measured and do not play a role. The reason the phase is not an observable in photodissociation is that the absorption cross section is proportional to the squared modulus of the dipole matrix element,

$$\sigma \propto |\langle g|D^{(j)}|E\rangle|^2 \tag{1}$$

where $|g\rangle$ and $|E\rangle$ are, respectively, a bound and a scattering wave function, E is the total scattering energy, and $D^{(j)}$ is the j-photon dipole operator. For a single-photon transition, $D^{(1)} = \mu\varepsilon$, where μ is the electronic dipole moment and ε is the electric field vector of the light source.

The phase of the transition dipole matrix element can lead to an observable effect if more than one pathway connecting the initial and final states is available. Because the amplitudes are added before the modulus is taken, cross terms arise that contain phase information. The phases involved might originate from the light fields used to generate the interfering paths, or they might be properties of the matter waves associated with the paths. Examples of both are presented in the following section. It is also possible to design experiments in which the phase of the cross term is produced both by the intrinsic phases of the matter waves and by the external phases of the electromagnetic field. In this case a powerful synergistic effect results in which the light phase may be used both to control the matter waves and to probe their properties. The information extracted from this synergism is the main topic of this paper, and is discussed in the third section. Specifically, we show that the relative phases of transition dipole elements, which can be measured by use of the phase property of light, contain a wealth of information that is not readily obtained by more conventional methods. Examples are couplings between continua, resonance properties, including the phase of a quasi-bound wave function, and spectroscopic properties of transitions that are not observed in the absorption spectrum. Illustrations of each of these are provided in section. 3.3, using the ionization and dissociation of hydrogen iodide as a working example. The final section summarizes our conclusions.

2. Interference Effects Produced by Matter and Light Waves

2.1. Interference of Matter Waves. We open this section with two textbook examples that illustrate how quantum mechanical interference between coherent paths produces a cross term containing the relative phases of the matter waves associated with each path. Consider first the elastic scattering of a particle having energy E and impact parameter b. The classical scattering cross section for deflection by an angle χ is given by[5]

$$I(\chi)\sin\chi = \frac{b}{|\mathrm{d}\chi/d\mathrm{b}|} \tag{2}$$

10.1021/jp003910b CCC: $20.00
Published on Web 04/17/2001

If the scattering potential is a repulsive function, $\chi(E,b)$ is a unique function of b, and semiclassical interference effects play no role.[6] If the potential has an attractive well, however, $\chi(E,b)$ is multivalued, so that more than one impact parameter leads to the same scattering angle. Corresponding to each impact parameter, b_j, is a unique trajectory and an associated phase shift, $\eta(E,b_j)$. This phase shift is essentially the difference between the number of radial deBroglie lengths along the actual trajectory and the corresponding number along a reference trajectory for which the potential has been turned off, in units of 2π. The semiclassical differential cross section is written as the square of the sum of the amplitudes associated with the various trajectories. For the case of two interfering paths, the cross section is thus[5]

$$I(\chi) = |I(b_1)^{1/2}e^{i\beta_1} + I(b_2)^{1/2}e^{i\beta_2}|^2 = I(b_1) + I(b_2) + 2[(I(b_1)I(b_2)]^{1/2}\cos(\beta_2 - \beta_1) \quad (3)$$

where

$$\beta_j = 2\eta(E,b_j)$$

up to a constant that depends on the curvature of the potential. The cosine term in eq 3 contains the phase information that we are seeking. From an analysis of the energy dependence of the cross term, it is possible to recover the potential energy function.

A second well-known example is Fano interference, which leads to asymmetric line shapes in bound-to-free transitions.[7] In this case, the two paths are direct photoexcitation of the target to the continuum state and an indirect transition to the continuum via an isolated resonance state that is coupled to the continuum. Again, we can write the cross section as the squared modulus of the sum of two amplitudes,

$$I = |f_d e^{i\delta_d} + f_r e^{i\delta_r}|^2 \quad (4)$$

where f_d is the modulus of the transition dipole matrix element for the direct path, δ_d is its argument, and f_r and δ_r are the corresponding quantities for the resonance-mediated path. It is shown in ref 8 that eq 4 is equivalent to the standard expression for a Fano line shape, which is characterized by a reduced energy variable, ϵ, and an asymmetry parameter, q. The phase for the direct path, $\exp(i\delta_d)$, is just the phase of the dipole matrix element for a j-photon process connecting the ground state with the continuum,

$$f_d^{(j)} e^{i\delta_d^{(j)}} = \langle g|D^{(j)}|E,\hat{k}_1\rangle \quad (5)$$

where $\hat{k}$ denotes the scattering angles.[9] The argument of the indirect path is the sum of three terms,

$$\delta_r^{(j)} = \delta_{gi}^{(j)} + \delta_{ic} + \delta_i \quad (6)$$

The terms in eq 6 are (i) the argument of the matrix element of the dipole operator connecting the ground state with the quasi-bound resonance, $|i\rangle$,

$$f_{gi}^{(j)} e^{i\delta_{gi}^{(j)}} = \langle g|D^{(j)}|i\rangle \quad (7)$$

(ii) the argument of the matrix element of a term in the molecular Hamiltonian, H_M, that couples the resonance to the continuum[10] (e.g., the spin−orbit operator),

$$f_{ic} e^{i\delta_{ic}} = \langle i|H_M|E,\hat{k}_1\rangle \quad (8)$$

and (iii) the Breit-Wigner phase of the resonance,

$$f_i e^{i\delta_i} = \{E - E_i - \Delta_i - i\Gamma_i\}^{-1} \quad (9)$$

where E_i is the unperturbed resonance center, and Δ_i and Γ_i are the shift and width of the resonance that are caused by interaction with the continuum. In terms of Fano's reduced energy and asymmetry parameters, we have

$$\cot \epsilon = -\delta_i \quad (10)$$

and

$$\cot q^{(j)} = \delta_{gi}^{(j)} \quad (11)$$

The cross term that results from taking the square in eq 4 contains the various matter phases defined in eqs 6−8. The dipole operator contains the phase of the electromagnetic field, but this phase is common to both the direct and indirect paths and cancels out of the final expression.

2.2. Interference Generated by Light Waves. We consider next a case where modulation of the interference term is produced by the relative phases of two light waves. Suppose that a molecule undergoes a bound-bound transition by simultaneously absorbing m photons of frequency ω_n and n photons of frequency ω_m, such that $m\omega_n = n\omega_m$. Suppose further that the electric fields are described by plane waves,

$$\varepsilon_{\mathbf{n}} = \boldsymbol{E}_{\mathbf{n}} e^{i(\omega_n t + \phi_n)} \quad (12)$$

where $\boldsymbol{E}_{\mathbf{n}}$ is the amplitude of field n, ω_n is the optical frequency, and ϕ_n is a constant phase. It is straightforward to show that the overall transition probability is given by[11]

$$P = P_m + P_n + 2P_{mn}\cos\phi \quad (13)$$

where P_m and P_n are the probabilities of absorbing n and m photons, the amplitude of the cross term is given by

$$P_{mn} = (P_m P_n)^{1/2} \quad (14)$$

and the relative phase is given by

$$\phi = m\phi_n - n\phi_m \quad (15)$$

We see in eq 13 that the cross term contains the relative phase of the light waves that generate the interfering paths. By experimentally varying ϕ, it is possible to control the population of the excited state. Because all the states involved in this case are assumed to be bound, their wave functions are real-arithmetic (up to an arbitrary phase) and therefore do not contribute a matter phase to the cross term.

An experimental demonstration of this result is shown in Figure 1. In this example,[12] a molecular beam of HCl molecules absorbed three UV photons of wavelength $\lambda_1 = 335.8$ nm and one vacuum UV (VUV) photon of wavelength $\lambda_3 = 111.94$ nm. The VUV photon was produced coherently from the UV by third harmonic generation in Kr gas. The relative phase of the laser beams was adjusted by passing them through a cell containing a variable pressure of H_2 gas. The difference in index of refraction of H_2 at the two wavelengths produced a phase difference that was proportional to the gas pressure and path length.[13] The electronically excited molecules were ionized by an additional UV photon and detected by a time-of-flight mass spectrometer. Variation of the H_2 pressure produced a modulation of the HCl^+ signal, as predicted by eq 13. This method of

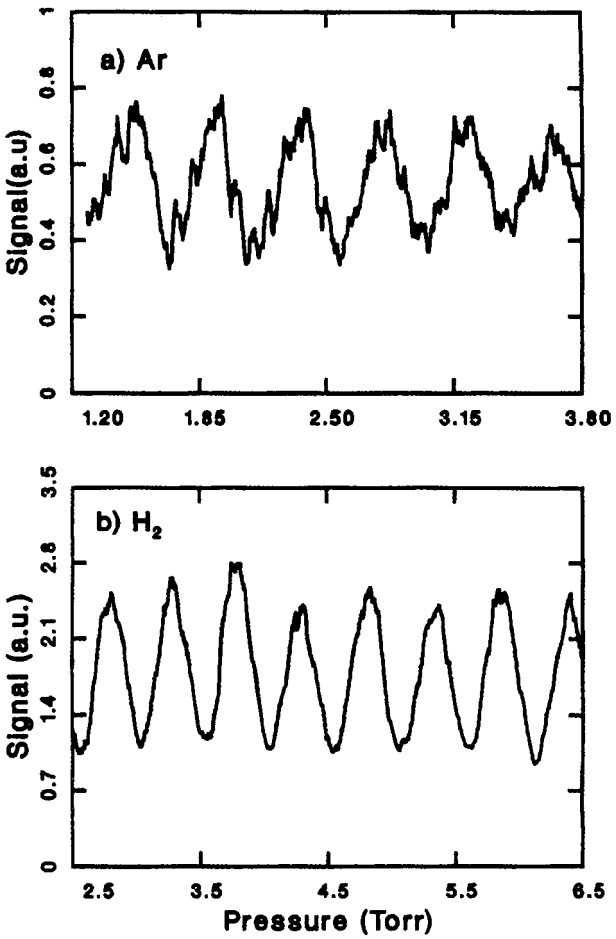

Figure 1. Modulation curve for the bound-bound $j^3\Sigma^-(\Omega=0^+,v'=0,J'=3)\leftarrow X^1\Sigma(v''=0,J''=2)$ transition of HCl, using either (a) Ar or (b) H_2 to control the relative phases of ω_1 and ω_3. Reprinted with permission from ref 12. Copyright 1998 American Institute of Physics.

controlling the excited-state population has been applied to atoms[14] as well as to large molecules.[15]

2.3. Limitations of Multipath Interference. The above illustrations show the utility as well as the limitations of multipathway excitation. The examples of matter wave interaction demonstrate how interference patterns may be used to determine system properties, such as the shape of the potential energy function in the case of elastic scattering and the resonance parameters in the case of Fano line shapes. The Fano problem also provides a means of controlling the reaction yield by simply tuning the excitation energy across the line shape.[16] But these examples also show that, if only natural interference is exploited, the opportunities both for extracting useful information about molecular continua and for controlling reaction pathways are very limited. For instance, the branching ratio between two decay channels can be controlled only if the associated Fano line shapes have a significantly different energy dependence. Clearly, no information about the phases of matrix elements is available if only a single route (direct or resonance-mediated) is present, and only little can be learned if both are present.

The example of multipathway bound-bound excitation shows how an external light phase can be used to modulate an excited-state population. Although this is a beautiful illustration of quantum mechanical interference, it neither addresses the chemical objectives of controlling reaction yields and product distributions nor does it provide information about the molecule beyond that available from conventional spectroscopy. In the following section we show that both objectives may be realized by multipathway bound-free photoexcitation to a degenerate continuum.

3. Interaction of Matter and Light Phases

3.1. Phase Lags and Channel Phases. Consider again the simultaneous excitation of a system with m photons of frequency ω_n and n photons of frequency m, only now let the excited state consist of two degenerate continua labeled by a channel index, S. The reaction probability for product channel S, integrated over scattering angles, is given by[11]

$$P^S = \int d\hat{k} |\langle g|D^{(m)} + D^{(n)}|E,S,\hat{k}\rangle|^2 \tag{16}$$

Expanding the square in eq 16, we obtain

$$P^S = P^S_m + P^S_n + 2P^S_{mn}\cos(\delta^S_{mn} + \phi) \tag{17}$$

where $P_{m(n)}$ is the single-path probability of obtaining product S by absorbing $n(m)$ photons, and the cross term is given by

$$P^S_{mn} e^{i\delta^S_{mn}} = e^{-i\phi}\int d\hat{k}\langle g|D^{(m)}|E,S,\hat{k}\rangle\langle E,S,\hat{k}|D^{(n)}|g\rangle \tag{18}$$

We refer to the quantity δ^S_{mn} as the *channel phase*. The key result is that the channel phase and the relative light phase appear together as a sum in the cross term. It is evident from eq 17 that to maximize the yield of product S one needs simply to set $\phi = -\delta^S_{mn}$. Moreover, one can use the light phase to extract information about the channel phase from the interference pattern.

An experimental example of the intertwining of matter and light phases is seen in the photoionization and photodissociation of HI,[17]

$$\mathrm{HI} + \omega_3, 3\omega_1 \rightarrow \mathrm{HI}^+ + e^-$$
$$\rightarrow \mathrm{H} + \mathrm{I}$$

Typical modulation data for both product channels are shown in Figure 2. The important point to note is that the modulation curves for the two channels are shifted with respect to one another by a *phase lag* $\Delta\delta(A,B)$, which is just the difference between two channel phases,

$$\Delta\delta(A,B) = \delta^A_{13} - \delta^B_{13} \tag{19}$$

In the example of Figure 2, $\Delta\delta(\mathrm{HI}^+,\mathrm{I}) = \delta^{\mathrm{HI}^+}_{13} - \delta^I_{13} = 150°$. Phase modulation of bound-free transitions has also been observed in the photodissociation of CH_3I,[18] the photoionization of H_2S,[19] and in the generation of photocurrents in an AlGaAs quantum well[20] and in amorphous GaAs;[21] however, in these experiments the channel phase was not observed. It is shown below that, once properly understood, δ_{13} may be extracted from a measurement of $\Delta\delta$.

The interest in the phase lag from the viewpoint of coherent control of product distributions is clear.[22] A priori one does not know if a given branching ratio would be controllable. Although in principle one may alter the branching ratio by varying only the intensities of the two fields, interpretation of the intensity-dependent product distribution can be ambiguous. A phase lag between two channel phases, however, is a clear hallmark of control. Perhaps still more important is the new information contained in δ_{mn} about molecular continua. To utilize the channel phase, both as a tool for control and as a route to molecular properties, it is essential first to explore the physical origin of

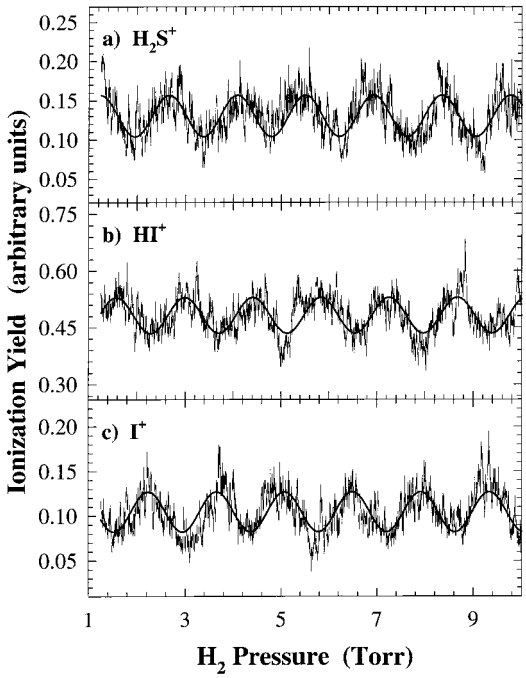

Figure 2. Modulation curves for H_2S^+, HI^+, and I^+ for a mixture of H_2S and HI. The wavelength of the ω_1 field is 353.80 nm. The period of the oscillation is determined by the refractive index of H_2 in the phase-tuning cell. Reprinted with permission from ref 40. Copyright 1999 Royal Society of Chemistry.

the channel phase and relate its properties to the structure of the underlying continuum. In the following subsection we examine the various mechanisms that produce a channel phase and summarize the characteristics of each one.

3.2. Physical Origin of the Phase Lag. The origin of the phase lag has been the subject of significant interest as well as controversy.[23,25,26] Early theoretical studies argued that this phase should vanish identically[23] (but see ref 24 for a resolution of the controversy) or that it may arise only from complex intermediates in the multiphoton process.[26] We now know that there are three general sources for a channel phase. These are (i) coupling of the exit channel continuum to some other continuum, (ii) the presence of a resonance embedded in the exit continuum, and (iii) the existence of a resonance at an intermediate energy, which contributes a phase to only one of the interfering paths. Elsewhere[27] we provide the link between the energy dependence of the channel phase and the properties of the continuum by re-expressing δ_{mn}^S of eq 18 in terms of physical (in principle observable) parameters, rather than in terms of the (usually unknown) eigenstates. Here we review only the end results of the theoretical analysis, with the help of a schematic drawing given in Figure 3.

In the limiting case of a single (i.e., uncoupled) continuum having a purely elastic potential energy, the channel phase vanishes exactly. This result, labeled case (a) in Figure 3, may be seen by expanding the continuum wave function in a partial wave series and noting that the phase shift of each partial wave cancels out in the integrated cross term.[8] The realization that certain processes produce no channel phase allows one to determine the channel phase of a process of interest by measuring the phase lag between the reaction of interest and one having a zero channel phase.

In the case that the product channel continuum is coupled to some other (possibly unobserved) continuum, the product wave function can be written as a linear combination of continuum functions,

$$|E,S,\hat{k}\rangle = a|E,S,A,\hat{k}\rangle + b|E,S,B,\hat{k}\rangle \quad (20)$$

Inserting this wave function into eq 18 yields a channel phase,

$$\delta_{13}{}^S = \arg\{\sum_{JM} C_A^{JM} + C_B^{JM} + C_{AB}^{JM}\cos(\delta_A^J - \delta_B^J)\} \quad (21)$$

where δ_A^J and δ_B^J are the partial wave phase shifts associated with the two continuum channels, and the C_S^{JM} are real arithmetic function (assuming that a and b are real) given in terms of the partial wave amplitudes $f_{EJM}^{(j)}$ defined in ref 8. We note that the phase that arises from the interference of smooth continuum channels, denoted as case (b) in Figure 3, varies only slowly with energy—on the scale of the deBroglie energy associated with the continua.

Another limiting scenario where the channel phase vanishes exactly is one in which the transition to the continuum occurs exclusively via a resonance-mediated path involving a single, isolated resonance. If there is no direct path to the continuum, the excitation and decay paths are completely uncoupled, and the channel phase vanishes,[27]

$$P_{mn}e^{i\delta_{mn}^S} = \int d\hat{k}\langle g|D^{(m)}|i\rangle \frac{|\langle i|H_M|ES\hat{k}_1^-\rangle|^2}{(E - E_i - \Delta_i)^2 + \Gamma_i^2/4}\langle i|D^{(n)}|g\rangle \quad (22)$$

If both resonance-mediated and direct paths contribute near the resonance and the continuum is elastic, then $|\delta_{mn}^S|$ will have a maximum near resonance, where two routes interfere (case (c)), falling to zero far from the resonance, where only a single route is available. In the limit where the initial state is prepared in a single rotational level, the channel phase in case (c) is given by a Lorentzian function,

$$\tan\delta_{mn}^S = \frac{2(q^{(m)} - q^{(n)})}{\left[\epsilon - \frac{1}{2}(q^{(m)} + q^{(n)})\right]^2 + \left[4 - \frac{1}{4}(q^{(m)} - q^{(n)})^2\right]} \quad (23)$$

which vanishes for $q^{(m)} = q^{(n)}$. If the continuum is coupled, however, then far from the resonance the direct path produces the slowly varying channel phase discussed above in case (b). The absolute value of the phase lag spectrum will then appear as a "window function", falling to a minimum near resonance (case (d)). Similarly, two or more coupled resonances can be shown to produce a nonvanishing phase, irrespective of the availability of a direct process.[8] In this case δ_{mn}^S arises from interference between the resonant pathways. This case is depicted schematically in Figure 3e. In the general case several sources of δ_{mn} are entangled, giving rise to more complex spectra. The case of two coupled resonances interacting with a coupled continuum is shown in panel (f).

The various control schemes involving at most a single resonance may be conveniently summarized in terms of a "four-slit" diagram. For purposes of illustration, we consider the specific example of one- vs three-photon excitation[28] and label the paths 1d, 1r, 3d, and 3r, as shown in Figure 4. Cases (a) and (b) utilize only direct excitation paths (1d and 3d), whereas cases (c−f) involve all four paths. In the example of a "window function" paths 1r and 3r dominate, causing the channel phase to vanish on resonance. The actual contributions of the various paths depend on the magnitudes of coupling matrix elements, so that it is possible to have, for example, a hybrid case consisting of three dominant paths.

In the above examples, the channel phase is caused by structured continua at an energy of $m\omega_n$ (e.g., at $3\omega_1$). A

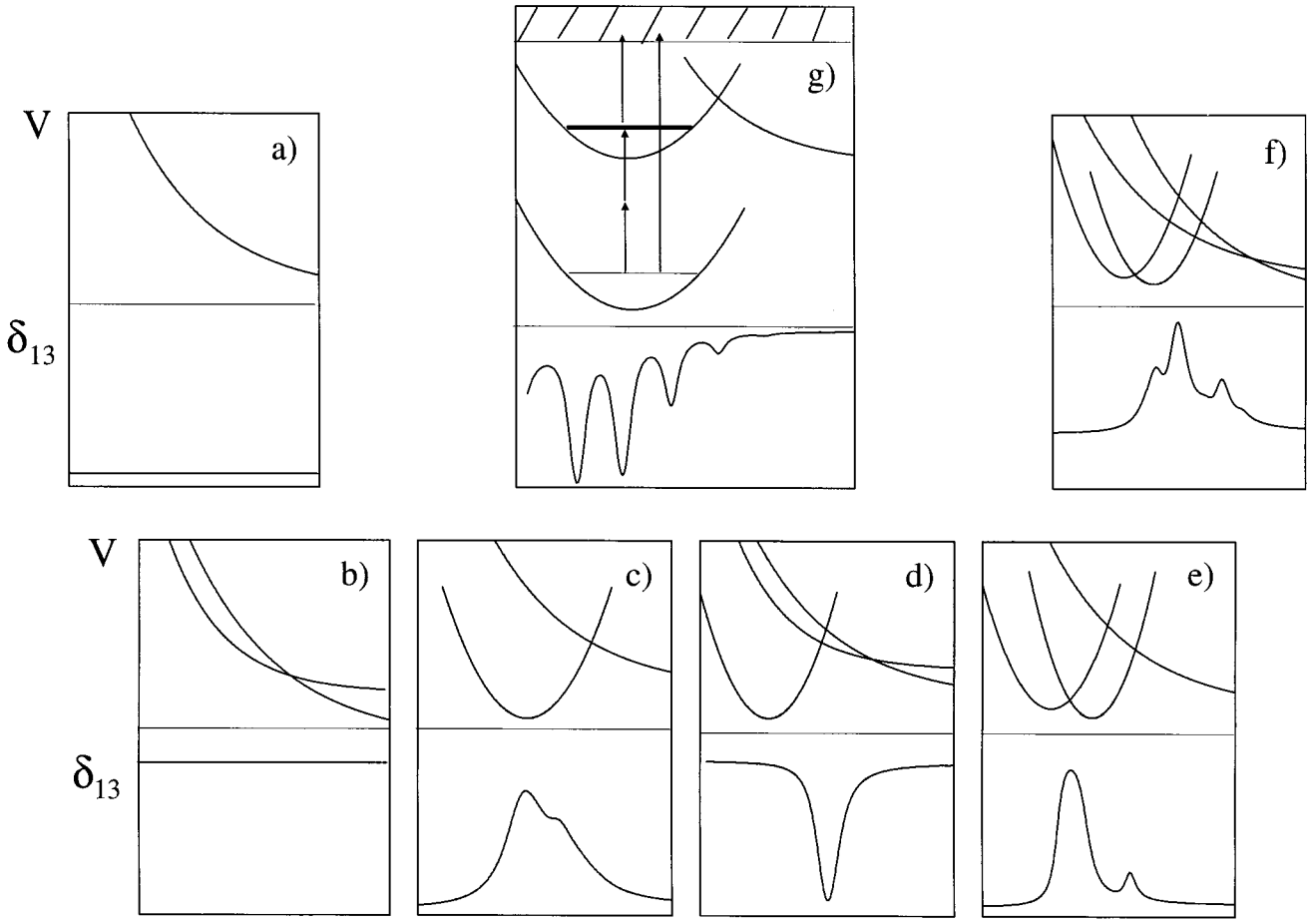

Figure 3. Schematic drawing showing different sources of a channel phase, δ_{13}^{S}. The various cases are discussed in the text.

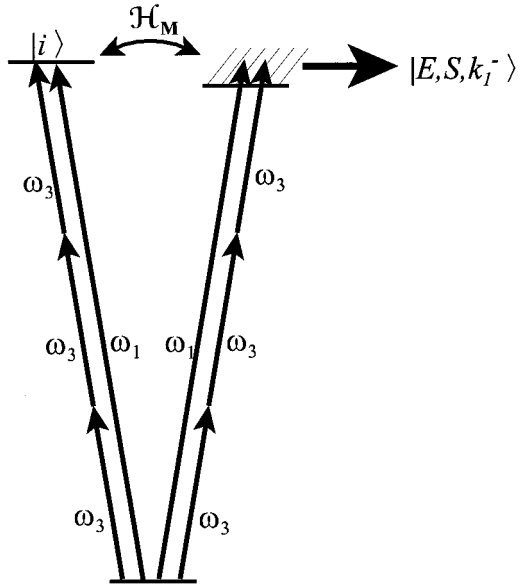

Figure 4. The "four-slit" mechanism for coherent control. The set of arrows on the right denote direct excitation to the dissociation or ionization continuum. The arrows on the left indicate resonance-mediated paths for either predissociation or autoionization of the molecule. H_M is a term in the Hamiltonian that couples the resonance state $|i\rangle$ to the continuum. Reprinted with permission from ref 43. Copyright 2000 American Institute of Physics.

qualitatively different interference effect arises if there happens to be a resonance at an intermediate level of excitation in the multiphoton process (e.g., at ω_1 or $2\omega_1$). This effect is illustrated pictorially in Figure 5. If the final state is elastic, and if there are no intermediate resonances, the channel phase is zero (as depicted on the left of Figure 5). The presence of a quasi-bound state at $2\omega_1$ (shown on the right) introduces a phase shift of $-\delta_{res}$, which is equal to the negative of the Breit−Wigner phase of the resonance. For a single rotational state having a rotational quantum number J_2 and an energy E_{J_2}, the Breit−Wigner phase is given by[29]

$$\delta_{res} = -\arg(E - E_{J_2}) = -\tan^{-1}[(\Gamma_{J_2}/2)/(E - E_{J_2}^R)] \qquad (24)$$

where $E_{J_2}^R$ and $\Gamma_{J_2}/2$ are the real and imaginary parts of E_{J_2}, respectively. In this case the phase lag provides a direct measure of the phase of the resonance wave function.

3.3. Experimental Studies of the Phase Lag. Many of the phenomena predicted in the previous subsection have been observed experimentally. Because all of these experiments were performed using HI and DI, it is helpful first to review some of the electronic properties of this molecule.[30−32] The equilibrium configuration of the ground ($X^1\Sigma^+$) state of HI is ($1\sigma^2 \ldots 9\sigma^2 1\pi^4 \ldots 5\pi^4 1\delta^4 2\delta^4$)$10\sigma^2 11\sigma^2 6\pi$,[4] which corresponds to a closed shell H^+I^- ionic structure.[33] Promotion of an electron from a 6π valence orbital to the 12σ antibonding orbital (nominally a transition from the hydrogen 1s to an iodine 5p orbital) generates the $a^3\Pi_i$ and $A^1\Pi$ repulsive valence states. (See Figure 6). Promotion instead of an electron from an 11σ valence orbital to the 12σ antibonding orbital produces the repulsive $t^3\Sigma^+$ and the bound $V^1\Sigma^+$ valence states. Promotion of these electrons to higher lying orbitals produces Rydberg states with either an $X^2\Pi_i(\sigma^2\pi^3)$ or an $A^2\Sigma^+(\sigma\pi^4)$ ionic core. Removal of an outer π electron produces the ground state $X^2\Pi_i$ ion. The ionization

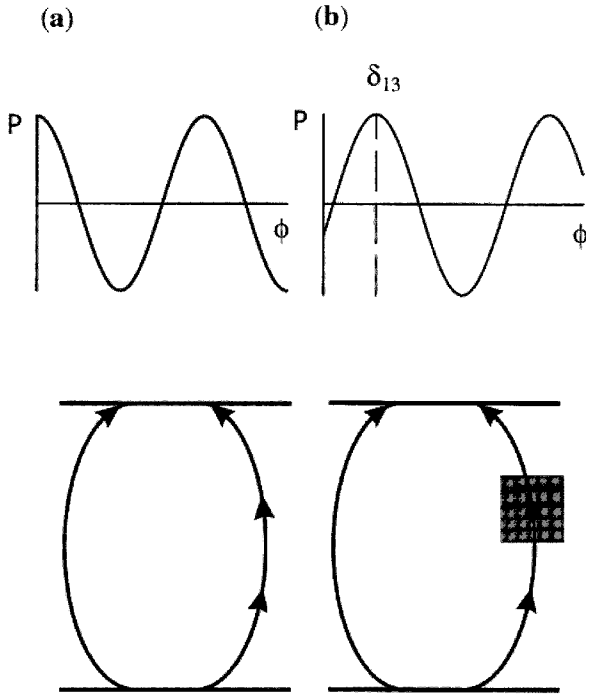

Figure 5. Illustration of a "molecular interferometer." Column (a) shows that two competing quantum mechanical paths connecting the same initial and final states produce a sinusoidal variation of the product signal that depends on the relative phase of the two paths. In column (b) an additional phase source is introduced at an intermediate level of the three-photon path. This source could be, for example, a predissociating resonance. The effect of this source is to produce a phase shift of δ_{13} in the signal. Reprinted with permission from ref 43. Copyright 2000 American Institute of Physics.

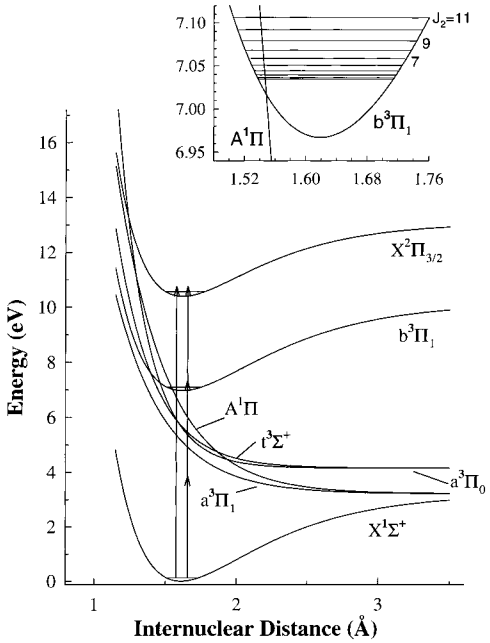

Figure 6. Excitation scheme of *HI*. One and three photons are used to produce ground state $HI^+(^2\Pi_{3/2})$ ions. The $b^3\Pi_1$ state, located near the two-photon level, is predissociated by several continuum states. The inset shows the rotational levels of the $b^3\Pi_1$, $v = 0$ state, which are predissociated by the $A^1\Pi$ continuum state. Reprinted with permission from ref 43. Copyright 2000 American Institute of Physics.

threshold lies at 83750 ± 1 cm^{-1},[34,35] and the spin−orbit excited $X^2\Pi_{1/2}$ state lies at 89109 ± 1 cm^{-1}.[36]

The potential energy curves relevant to this subsection are sketched in Figure 6. Phase lag measurements were performed

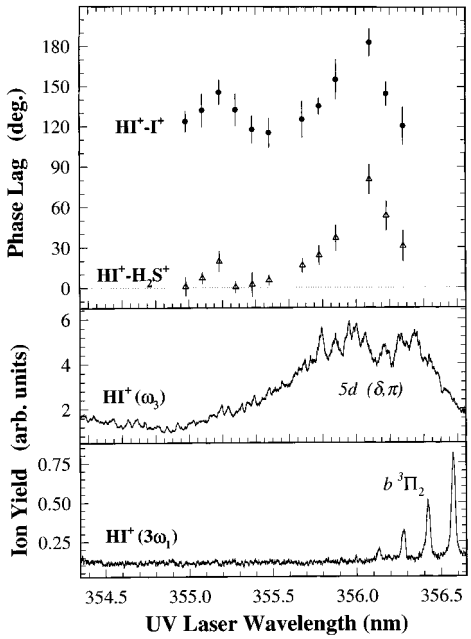

Figure 7. Phase lag spectrum (top part) for the photodissociation and photoionization of HI (circles) and for the photoionization of a mixture of HI and H_2S (triangles) in the vicinity of the $5d(\pi,\delta)$ resonance of HI. The bottom two panels are the one-and three-photon ionization spectra of HI. Reprinted with permission from ref 40. Copyright 1999 Royal Society of Chemistry.

in the energy regime 84200−85020 cm^{-1}, which lies slightly above the first ionization threshold. Twelve Rydberg series converging to the $X^2\Pi_{1/2}$ ion have been assigned.[37,38] Our studies involved two of the lowest states in these Rydberg series, namely, the $5s\sigma$ and the $5d(\pi,\delta)$ states.[39] At approximately two-thirds of the ionization potential lie the $b^3\Pi_2$ and $b^3\Pi_1$ states, which are the two lowest Rydberg states of HI. These states can be utilized to explore the effect of complex intermediates on the phase lag (Figure 3g) by tuning the energy of the three-photon beam to half the $b^3\Pi_i$ resonance energy.

As discussed in the previous subsection, it is impossible to tell from measurements of $\Delta\delta(HI^+,I)$ alone whether ionization or dissociation (or both) is (are) responsible for the observed phase difference between the signals. Having shown, however, that for specific, well-defined processes the phase shift vanishes rigorously, we can use such a process as a reference to determine the absolute phase shift of another process. In our experiments we chose as the reference channel the ionization of H_2S, which was co-expanded with HI (or DI) in the molecular beam.

Figure 7 shows the phase lag spectrum of HI in the vicinity of the $5d(\pi,\delta)$ Rydberg state,[40] illustrating various aspects of cases (a), (b), and (c). The $\Delta\delta(HI^+,H_2S^+)$ phase lag, obtained from a mixture of HI and H_2S, displays a maximum at 356.1 nm, in the vicinity of the resonance, as well as a secondary maximum at 355.2 nm. These peaks ride on a baseline of approximately zero, which is indicative of elastic continua for ionization of both molecules, in accord with case (a). In contrast, the channel phase for dissociation of HI (obtained from $\Delta\delta(I,H_2S^+)$) varies weakly with energy between $-90°$ and $-120°$, indicating that the dissociative continuum is inelastic (case (b)). Although the maximum near 356.1 nm is almost certainly associated with the 5d resonance, the detailed mechanism is a bit complicated. In principle the overlapping $5d\pi$ and $5d\delta$ resonances produce in this case interference of type (e). Because, however, the three-photon resonant route is very weak, only three routes, 1r + 1d + 3d, contribute in practice.

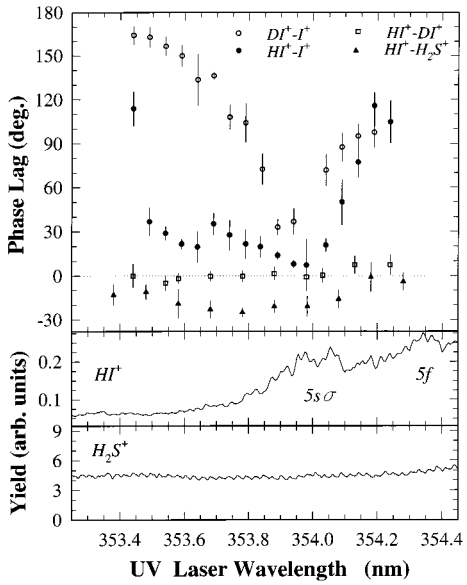

Figure 8. Phase lag spectrum (top part) for the photodissociation and photoionization of HI and DI in the vicinity of the 5sσ resonance of *HI*. The solid circles denote the phase lag, $\Delta\delta(HI^+,I)$, between the ionization and dissociation channels of HI. The open circles denote the corresponding phase lag, $\Delta\delta(DI^+,I)$, for DI. The open squares denote $\Delta\delta(HI^+,DI^+)$ for the ionization of a mixture of HI and DI, and the solid triangles denote $\Delta\delta(HI^+,H_2S^+)$ for the ionization of a mixture of HI and H_2S. The bottom two panels are the one-photon ionization spectra of HI and H_2S. Reprinted with permission from ref 42. Copyright 1999 American Institute of Physics.

(The sharp structure in the three-photon resonance in the bottom panel of Figure 7 corresponds to rotational structure in the two-photon $b^3\Pi_2$ resonance.)

An example of case (d) is shown in Figure 8.[41] Here $\Delta\delta(DI^+,I)$ has a deep minimum near the 5sσ resonance, which is indicative of a resonance embedded in an inelastic continuum.The data also show a striking isotope effect, which is still under investigation. To determine which continuum (ionization, dissociation, or both) is responsible for this effect, we co-expanded a mixture of HI and DI and measured the interisotope phase lag, $\Delta\delta(HI^+,DI^+)$. The vanishing of this quantity across the 5sσ resonance (Figure 9[42]) proved that the isotope effect is caused entirely by the dissociation channel.A measurement of $\delta(HI^+,H_2S^+)$ for an HI/H_2S mixture revealed a maximum in the absolute value of the phase lag near the resonance,[42] which is again indicative of a resonance embedded in an elastic ionization continuum (case (b).

We turn now to a case of a quasibound state at an intermediate level of excitation, which is depicted schematically in Figure 5g. Using the ionization of H_2S^+ as a reference proved again to be a valuable technique. The origin of the $b^3\Pi_1 \leftarrow X^1\Sigma^+$ transition lies at 56738.3 cm^{-1},[30] which is just slightly greater than two-thirds of the ionization threshold of HI. Figure 9[43] reveals rotational structure in $\Delta\delta(HI^+,H_2S^+)$ that is caused by predissociation of $b^3\Pi_1(v_2=0,J_2=5-7)$. Because the molecular beam is not very cold, many rotational levels of HI are populated. For a thermally averaged parent state, eq 24 generalizes as

$$\tan \delta_{13}^S = \frac{\sum_{J_g J_2} A_{J_g,J_2} \Gamma_{J_2}[(E_{J_g} + 2\omega - E_{J_2}^R)^2 + \Gamma_{J_2}^2/4]^{-1}}{2\sum_{J_g J_2} A_{J_g J_2}(E_{J_g} + 2\omega - E_{J_2}^R)[(E_{J_g} + 2\omega - E_{J_2}^R)^2 + \Gamma_{J_2}^2/4]^{-1}} \quad (25)$$

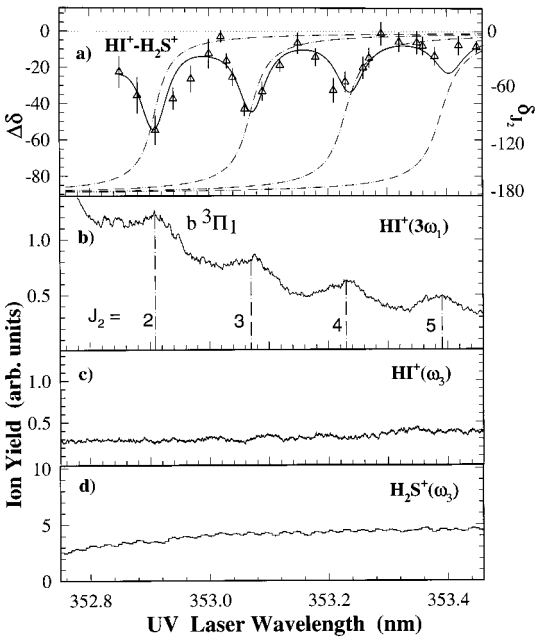

Figure 9. Phase lag and ionization spectra of HI and H_2S dominated by the $b^3\Pi_1$ resonance of HI at the two-photon level. Part (a) shows the observed phase lag between the HI^+ and H_2S^+ signals. Error bars are a single standard deviation. The solid and dot−dashed curves are explained in the text. Part (b) is the three-photon UV ionization spectrum of HI, showing the two-photon, O-type rotational branch (indicated by vertical dot−dashed lines) of the $b^3\Pi_1(v_2=0,J_2)X^1\Sigma^+(v_g=0,J_g)$ transition. Parts (c) and (d) show the one-photon VUV ionization spectra of HI and H_2S, respectively. Reprinted with permission from ref 43. Copyright 2000 American Institute of Physics.

where A_{J_g,J_2} is a multiple sum over products of dynamical, geometric, and Boltzmann weighting factors, given explicitly in ref 27. Making the single (and common[44]) approximation in eq 25 that the body-fixed eigenfunctions and the corresponding eigenvalues are independent of the total angular momentum, one arrives at an analytical expression for the channel phase that does not rely on knowledge of the electronic structure of the molecule. The solid curve in the top panel of Figure 9 is a least-squares fit of this function to the data, in which the resonance width and rotational beam temperature are treated as adjustable parameters. The Breit−Wigner phase of individual rotational resonances extracted from the fit are shown by the dot−dashed curves. Allowing up to a linear dependence of the resonance width on J_2, we find a rotational temperature of 236 K and $\Gamma_{J_2} = (5.5 + 0.61J_2)$ cm^{-1}. The increase of Γ_{J_2} with J_2 is indicative of a rotational perturbation coupling the $b^3\Pi_1$ state to the continuum and is consistent with our spectroscopic observation that the branching ratio of predissociation vs ionization increases with J_2.

4. Concluding Remarks

Our initial interest in the phase lag was sparked by its usefulness as a tool for controlling the branching ratios of chemical reactions. Equally engaging is the realization that the phase lag contains fundamental information about the continuum properties of molecules that cannot be obtained by conventional methods.

In the present work we discussed the various physical sources of a channel phase in a general molecular photoinitiated reaction and established a link between the energy dependence of the observable and the structure of the underlying continuum. These general concepts were exemplified though detailed experimental

studies of the competing ionization and dissociation processes of HI. At large detuning from autoionizing and predissociating resonances, $\delta^S_{mn}(E)$ provides dynamical information pertaining to the scattering portion of the continuum. Near resonance it provides short range, spectroscopic information. In energy regimes where quasibound states are accessed at an intermediate level of excitation, the channel phase provides a direct route to the Breit−Wigner phase of the resonance.

The former, long range, type of information is similar to that extractable from vector correlation measurements of photodissociation reactions.[45,46] In this regime the channel phase reflects the advancement or retardation of the deBroglie waves, producing changes in the scattering phase shift, $\eta(E,b_j)$, that are sensitive to the shape of the potential energy surface in the asymptotic region. The latter, short-range information suggests a new type of spectroscopy that may complement conventional (i.e., modulus-based) spectroscopies.

The possibility of using the phase property of light to infer matter phases suggests a range of exciting opportunities, the assessment of which will be the focus of future experimental and theoretical studies. One obvious, but potentially powerful, application, currently under investigation, is the detection of weak spectroscopic transitions that are not revealed by the modulus of the cross section, possibly because of a large background absorption. We have observed several maxima in the phase lag spectrum, such as the secondary peak at 355.2 nm in Figure 7, that are not clearly associated with any structure in the corresponding absorption spectrum. Another exciting possibility, explored in an ongoing theoretical study, is that of formulating a true inversion scheme based on the phase-sensitive data. Finally, the extension of our study to other systems, including polyatomic molecules, is expected to furnish new insights into the channel phase problem.

Acknowledgment. We wish to thank the National Science Foundation for its generous support of this research.

References and Notes

(1) Weinacht, T. C.; Ahn, J.; Bucksbaum, P. H. *Phys. Rev. Lett.* **1998**, *80*, 5508.

(2) Uberna, R.; Amitay, Z.; Loomis, R. A.; Leone, S. R. *Discuss. Faraday Society* **1999**, *113*, 385.

(3) Shapiro, M.; Brumer, P. *Adv. At. Mol. Opt. Phys.* **1999**, *42*, 287.

(4) Gordon, R. J.; Zhu, L.; Seideman, T. *Acc. Chem. Res.* **1999**, *32*, 1007.

(5) Child, M. S. *Molecular Collision Theory*; Dover: Mineola, 1974.

(6) If we allow b to be complex, there will be multiple interfering paths that produce oscillations in the differential cross section, in fairly good agreement with a full quantum mechanical treatment. See, for example, Gordon, R. J. *J. Chem. Phys.* **1975**, *63*, 3109.

(7) Fano, U. *Phys. Rev.* **1961**, *124*, 1866.

(8) Seideman, T. *J. Chem. Phys.* **1998**, *108*, 1915.

(9) The subscript 1 to the ket in eq 5 is introduced in ref 8 to distinguish the eigenstates of the complete Hamiltonian, *H*, (cf. eq. 16) from the eigenstates of the scattering portion of *H*, conventionally denoted PHP, i.e., a Hamiltonian from which the bound component has been projected out.

(10) H_M is the total molecular Hamiltonian, but only the interaction term in it has nonvanishing matrix element between $\langle i|$ and $|E,\hat{k}_1\rangle$.

(11) Brumer, P.; Shapiro, M. *Faraday Discuss.* **1986**, *82*, 177.

(12) Park, S. M.; Lu, S. P.; Gordon, R. J. *J. Chem. Phys.* **1998**, *108*, 1915.

(13) Gordon, R. J.; Lu, S.-P.; Park, S. M.; Trentelman, K.; Xie, Y.; Zhu, L.; Kumar Meath, W. J. *J. Chem. Phys.* **1993**, *98*, 9481.

(14) Chen, C.; Yin, Y. Y.; Elliott, D. S. *Phys. Rev. Lett.* **1990**, *64*, 506.

(15) Wang, X.; Bersohn, R.; Takahashi, K.; Kawasaki, M.; Kim, H. L. *J. Chem. Phys.* **1996**, *105*, 2992.

(16) Reid, S. A.; Brandon, J. T.; Reisler, H. *J. Phys. Chem.* **1993**, *97*, 540.

(17) Zhu, L.; Kleiman, V.; Li, X.; Lu, S.; Gordon, R. J. *Science* **1995**, *270*, 77.

(18) Kleiman, V. D.; Gordon, R. J. *J. Chem. Phys.* **1994**.

(19) Kleiman, V. D.; Gordon, R. J. *J. Chem. Phys.* **1994**.

(20) Dupont, E.; Corkum, P. B.; Liu, H. C.; Buchanan, M.; Wasilewski, Z. R. Z. R. *Phys. Rev. Lett.* **1995**, *74*, 3596.

(21) Haché, A.; Kostoulas, Y.; Atanasov, R.; Hughes, J. L. P.; Sipe, J. E.; van Driel, H. M. *Phys. Rev. Lett.* **1997**, *78*, 306.

(22) Gordon, R. J.; Rice, S. A. Annu. *Rev. Phys. Chem.* **1997**, *48*, 601.

(23) Lefebvre-Brion, H. *J. Chem. Phys.* **1997**, *106*, 2544.

(24) Lefebvre-Brion, H.; Seideman, T.; Gordon, R. J. *J. Chem. Phys.* **2001**, in press.

(25) Nakajima, T.; Zhang, J.; Lambropoulos, P. *J. Phys. B* **1997**, *30*, 1077.

(26) Lee, S.; *J. Chem. Phys.* **1997**, *107*, 2734.

(27) Seideman, T.; *J. Chem. Phys.* **1999**, *111*, 9168.

(28) Shapiro, M.; Hepburn, J. W.; Brumer, P. *Chem. Phys. Lett.* **1988**, *149*, 451.

(29) Sakurai, J. J. *Modern Quantum Mechanics*; Addison-Wesley: Reading, 1995.

(30) Tilford, S. G.; Ginter, M. L.; Bass, A. M. *J. Mol. Spectrosc.* **1970**, *34*, 327.

(31) Alekseyev, A. B.; Liebermann, H.-P.; Kokh, D. K.; Buenker, R. J. *J. Chem. Phys.* **2000**, *113*, 6174.

(32) Liyanage, R.; Gordon, R. J.; Field, R. W. *J. Chem. Phys.* **1998**, *109*, 8374.

(33) Ungemach, S. R.; Schaefer, H. F., III.; Liu, B. *J. Mol. Spectrosc.* **1977**, *66*, 99.

(34) Chanda, A.; Ho, W. C.; Dalby, F. W.; Ozier, L. *J. Chem. Phys.* **1995**, *102*, 8725.

(35) The ground-state ionization potential was calculated by subtracting the spin−orbit splitting reported in ref 34 from the ionization potential of the spin−orbit excited molecule reported in ref 36.

(36) Pratt, S. T.; *J. Chem. Phys.* **1994**, *101*, 8302.

(37) Hart, D. J.; Hepburn, J. W. *Chem. Phys.* **1989**, *129*, 51.

(38) Mank, A.; Drescher, M.; Huth-Fehre, T.; Böwering, N.; Heinzemann, U.; Lefebvre-Brion, H. *J. Chem. Phys.* **1991**, *95*, 1676.

(39) The labels 5sσ and 5d(π,δ) refer to the effective quantum numbers of the Rydberg electron, $n^*l\lambda$. They should not be confused with the sequential numbering of the molecular orbitals, as in the $10\sigma^2 11\sigma^2 6\pi^4$ ground-state configuration.

(40) Fiss, J. A.; Khachatrian, A.; Zhu, L.; Gordon, R. J.; Seideman, T. *Discuss. Faraday Society* **1999**, *113*, 61.

(41) Zhu, L.; Suto, K.; Fiss, J.; Wada, R.; Seideman, T.; Gordon, R. J. *Phys. Rev. Lett.* **1997**, *79*, 4108.

(42) Fiss, J. A.; Zhu, L.; Gordon, R. J.; Seideman, T. *Phys. Rev. Lett.* **1999**, *82*, 65.

(43) Fiss, J. A.; Khachatrian, A.; Truhins, K.; Zhu, L.; Gordon, R. J.; Seideman, T. *Phys. Rev. Lett.* **2000**, *85*, 2096.

(44) McClain, W. M.; Harris, R. A. In *Excited States*; Lim, E. C., Ed.; Academic: New York, 1977; Vol. 3, pp 1−56.

(45) Rakitzis, T. P.; Kandel, S. A.; Alexander, A. J.; Kim, Z. H.; Zare, R. N. *Science* **1998**, *281*, 1346.

(46) Bracker, A. S.; Wouters, E. W.; Suits, A. G.; Vasyutinskii, O. S. *J. Chem. Phys.* **1999**, *110*, 6749.